Smart Link Adaptation and Scheduling for IIoT

Miroslav Mitev, M. Majid Butt, Philippe Sehier, Arsenia Chorti, Luca Rose, Arto Lehti

Abstract—A machine learning enabled link adaption (LA) and scheduling framework is presented for industrial Internet of things (IIoT), leveraging quasi-periodicity of traffic in IIoT. The following steps are introduced: i) a reduced complexity link establishment accounting jointly for beamforming and load management; ii) interference prediction using long short-term memory neural networks; iii) semi-coordinated scheduling based on node grouping for interference avoidance. Through numerical evaluation it is demonstrated that the proposed approach can substantially improve average spectral efficiency by as much as 62% in a realistic IIoT scenario at negligible overhead.

Index Terms—Industrial IoT, link adaptation, scheduling, ML

I. INTRODUCTION

While industrial Internet of things (IIoT) is a key vertical in fifth generation systems and beyond (B5G), increased traffic in such environments poses challenges in terms of interference management and efficient spectrum usage [1]. Existing IIoT interference mitigation solutions, such as periodic and pseudo-random channel hopping [2], leverage the use of link adaptation (LA) techniques based on sounding reference signals in the uplink. This allows next generation Nodes B (gNBs) to periodically obtain channel state information (CSI) and update their modulation and coding scheme (MCS) in the downlink [3]. However, existing LA and scheduling approaches do not account for quasi-periodicity of traffic in IIoT environments [4], rendering it partially predictable [5], [6]. Incorporating interference prediction within the scheduling process can naturally improve the spectral efficiency (SE) [7].

In earlier works [7], centralized interference prediction and scheduling was proposed with coordination achieved at the cost of increased communication overhead. Alternatively, in the present work, traffic patterns are learned using distributed interference prediction using long short-term memory (LSTM) neural networks. The acquired knowledge is then used to drive a smart LA and scheduling framework that increases both fairness and SE, without extra communication overhead.

The proposed approach is evaluated in a realistic scenario that incorporates statistical traffic modelling, beamforming, 3GPP IIoT propagation models and user equipment (UE) attachment optimization. Our contributions are listed below:
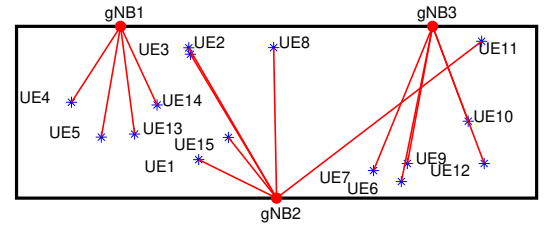
- A UE attachment algorithm that increases the number of UEs served within the network.
- Machine learning (ML) based interference prediction which allows gNBs to adaptively adjust their MCS.

M. Mitev is with Barkhausen Institut gGmbH, Dresden, Germany (miroslav.mitev@barkhauseninstitut.org);
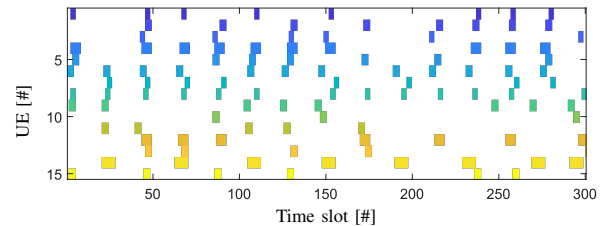
M. Butt, P. Sehier, L. Rose, and A. Lehti are with Nokia Bell Labs, 91620 Paris, France ({majid.butt, philippe.sehier, luca.rose, arto.lehti}@nokia-bell-labs.com);

A. Chorti is with ETIS UMR8051, CYU, ENSEA, CNRS, F-95000, Cergy, France (arsenia.chorti@ensea.fr);

gNB1 · UE3 · UE2 · UE8 · gNB3 · UE11 · UE4 · UE14 · UE5 · UE13 · UE10 · UE15 · UE1 · UE9 · UE12 · UE7 · UE6 · gNB2

a) System model.

b) Generated traffic for 15 UEs, each shown in different color.

Fig. 1: Traffic model.

- Semi-coordinated scheduling approach that substantially increases the average SE compared to standard practises.

To the best of our knowledge, this is the first work that proposes to combine interference prediction and semi-coordinated scheduling in a LA approach. The paper is organized as follows: the system model is presented in Section II. The proposed smart LA and interference aware semi-coordinated scheduling is presented in Section III, numerical results in Section IV and conclusions in Section V.

II. SYSTEM MODEL

IIoT traffic patterns used in this study follow 3GPP specifications [4]. In detail, 10-20 UEs are simulated with message sizes of 20 Bytes, transfer intervals in the range of 10 msec (with variation upper bounded by ±5%) and a service area less than $100m \times 100m \times 50m$.[1] As illustrated in Fig. 1(a), in this work an IIoT setting with multiple gNBs generating downlink traffic flows is considered. The generated traffic is characterized by homogeneous asynchronous periodicity, i.e., the transfer intervals T_j for $j \in \mathcal{J}$ with $\mathcal{J} = \{1, \ldots, J\}$, defined here as the number of time slots between consecutive transmissions for each UE, are independent and identically distributed; the UEs received transmissions at independent start times s_j; the activation probability and transmission duration for each UE are denoted by $\beta_j \in [0, 1]$ and d_j, respectively, where d_j denotes number of time slots required for the transmission. In the above setting, messages to a single UE j are transmitted in slots $m = 1, 2, \ldots$, each with duration $[\tau_{j,m}, \tau_{j,m} + d_j]$, where:

$$\tau_{j,m} = B_j \left(s_j + (m-1)T_j \right), \tag{1}$$

---

[1]While these parameters are used in the simulations in Section IV, the proposed approach can be applied to any scenario with quasi-periodic traffic.
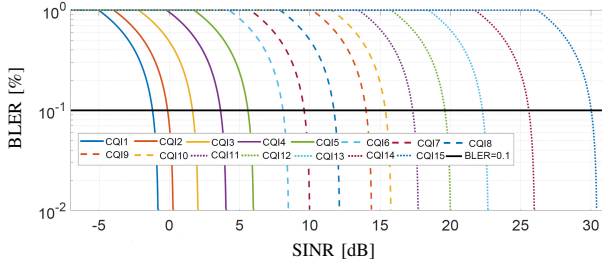
Fig. 2: BLER - CQI mapping defined as "Table-1".

where $B_j \sim \text{Bernoulli}(\beta_j)$. Fig. 1(b) illustrates generated traffic for $J = 15$ UEs. It is observed that different UEs have packets of different length and further, due to unequal probabilities of activation, some of them receive traffic in a periodic manner while others are rarely active.

With respect to the propagation model, the considered path-loss and shadowing models are as defined in the 3GPP TS 38.901 [8], Tables 7.2-4, 7.4.1-1 and 7.4.2-1. The model accounts for line of sight (LoS) and non-LoS, LoS probability, clutter density and size, antenna height, path-loss and shadowing. While a gNB serves a particular UE, it causes interference to other active UEs in the area. In this work, it is assumed that gNBs transmit with constant power P, as is common in literature. It is important to note that while power control can be employed to increase performance [9], such schemes are not part of relevant standards [10] and are not considered in this work. The signal to interference plus noise ratio (SINR) at the j-th UE attached to the i-th gNB, $j \in \mathcal{J}$ and $i \in \mathcal{I}$ with $\mathcal{I} = \{1, \ldots, I\}$, can be expressed as

$$SINR_j^{(i)} = \frac{PG_{i,j,\theta_j}L_{i,j}}{\sum\limits_{i^* \neq i} \sum\limits_{j^* \neq j} PG_{i^*,j,\theta_{j^*}}L_{i^*,j} + \sigma^2}. \qquad (2)$$

Note that the denominator represents the interference generated by gNBs serving other UEs, while G_{i,j,θ_j} is the antenna gain for the link gNB i - UE j when the tilt angle θ_j is pointing towards UE j; $L_{i,j}$ denotes path-loss for the link gNB i in the direction of UE j, respectively. Similarly, $G_{i^*,j,\theta_{j^*}}$ is the antenna gain for the link gNB i^* - UE j when the tilt angle θ_{j^*} is pointing towards UE j^* and $L_{i^*,j}$ denotes the path-loss for the link gNB i^* - UE j, finally, σ^2 denotes the variance of additive Gaussian noise.

Finally, a standard proportional fair scheduler is assumed, as described in [3], with the following parameters: i) $\overline{R}_{j,t}$ - past average rate for UE j at scheduling interval t; ii) $R_{j,t}$ estimated achievable rate for UE j, at current scheduling interval t. Priority is given to the UE with the highest fairness metric, given by $\frac{R_{j,t}}{\overline{R}_{j,t}}$; $\overline{R}_{j,t}$ is updated using a moving average filter:

$$\overline{R}_{j,t} = \left(1 - \frac{1}{N_{TTI}}\right)\overline{R}_{j,t-1} + \frac{1}{N_{TTI}}R_{j,t}, \qquad (3)$$

where N_{TTI} defines the length of the filter. It is assumed that each gNB has a single antenna panel and due to low power capabilities only one beam can be generated at a time. For simplicity, the system model considered in this study does not allow for frequency multiplexing and therefore, each AP can serve only a single UE at a time. Finally, all UEs are assumed

---

Algorithm 1: Heuristic Algorithm - UE attachment

1 For all UEs, identify attachment candidates from I gNBs within $\theta \in [-\gamma^\circ, \gamma^\circ]$;
2 Attach UEs to the gNB with smallest path-loss;
3 **if** $Load_i < 1 \forall i$ satisfied **then**
4   Keep attachment;
5 **else**
6   **for** *For gNBs $i \in \mathcal{I}$ where $Load_i > 1$* **do**
7   Sort attached UEs based on path-loss in descending order in a queue Q;
8   **for** *HOL UE $q \in Q$* **do**
9   **if** *There exists at least one gNB $\in \mathcal{I}$ with Load < 1 (including load from UE q) and $\theta \in [-\gamma^\circ, \gamma^\circ]$* **then**
10   Attach HOL UE with the gNB with smallest load and remove UE from Q;
11   **end**
12   **if** *$Load_i < 1$ for gNB i* **then**
13   Break;
14   **end**
15   **end**
16   **while** *$Load_i > 1$* **do**
17   Remove UEs from Q starting from HOL
18   **end**
19   **end**
20 **end**

---

to have the same delay constraints. In practice IIoT applications are heterogeneous with different delay requirements [11], which will be addressed in future work.

Finally, the block error rate (BLER) curves are generated based on MCS as defined in the 3GPP TS 38.214 [10]. The channel quality indicator (CQI) is reported by the UE to the gNB, as a part of the CSI; the CQI index takes values from 0 to 15, where higher values represent higher MCS. Depending on the BLER target and maximum modulation order, different mapping tables are used to transform CQI to MCS. This is defined by the higher layer parameter CQI-Table. In Fig. 2 the CQI mapping is illustrated for BLER$= 10^{-1}$ when selecting Table 1 parameters in [10].

III. SMART LINK ADAPTATION AND SCHEDULING

To optimally determine MCSs, continuous, real-time reporting of SINR levels from the UEs to gNBs would have been required (at unsustainably high communication overhead). In practise (baseline approach), gNBs *periodically* choose MCSs using only *average* SINR reports from the UEs. To fill this gap, a combination of smart LA and semi-coordinated scheduling is proposed, to boost the achievable SE while keeping the communication overhead low, leveraging the fact that IIoT traffic patterns can be used for interference prediction.

A. Attachment and ML based interference prediction

The first step in the smart LA is the attachment of UEs to gNBs. This is a combinatorial search problem and in order to reduce complexity a heuristic is proposed, given in

Algorithm 1. The algorithm accounts for path-loss, steering angle and sum load of gNBs. With respect to the steering angle, the number of antennas at the gNBs determines the shape and power concentration of interference patterns due to beamforming side and grating lobes. Grating lobes appear as a consequence of antenna spacing and steering angle.

Furthermore, in order to avoid buffer overflows, the queue lengths at each gNB should not be overloaded. Consequently, a condition captured in the i-th gNB's load as follows:

$$\text{Load}_i = \sum_{j \in \mathcal{J}} \mathbb{1}_{\{\mathbf{A}_{i,j}\}} \beta_j d_j T^{-1} \leq 1, i \in \mathcal{I}, \quad (4)$$

where $\mathbf{A}_{i,j}$ represents the logical proposition that UE j is attached to gNB i and $\mathbb{1}_{\{\mathbf{x}\}}$ is the indicator function while all other quantities are defined in Section II.

Initially, the gNB candidates satisfying the steering angle requirement for each UE are identified (line 1 in Algorithm 1). Next, path loss based attachment is performed (lines 2-4); however, if the load condition for a particular gNB is not satisfied, some of the UEs are offloaded to other gNBs based on load and angle conditions (lines 5-15). Finally, line 17 in Algorithm 1 captures buffer overflows (by dropping head of line (HOL) packets) in scenarios where the sum traffic exceeds the sum load capacity of the gNB and attachment to other gNB is not possible. Compared to traditional attachment algorithms, where UEs attach to the gNB with the highest received power [12], Algorithm 1 introduces a trade-off as a larger number of UEs can be served with negligible loss in terms of average throughput. As will be shown in the next section, if Algorithm 1 is employed in combination with the interference aware scheduler, throughput losses can be compensated while reducing the number of packets dropped. The complexity of Algorithm 1 is upper bounded by $O(I \log I)$, because of the sorting operation.

Following the initial attachment, interference prediction and CQI correction is executed. Interference prediction is performed using LSTM neural networks while a simple deterministic mapping is proposed for CQI correction, given in Algorithm 2. Note that Algorithm 2 is performed offline and outputs a mapping function which is used online to improve performance. In step 1, a LSTM neural network is used to predict the SINR experienced at different UEs over time. Then, using the BLER curves from Fig. 2, the predicted values are converted to their corresponding CQI index. The use of LSTM in this work is motivated by their ability to capture temporal dynamics, e.g., for traffic prediction [13]. Depending on the system model different LSTM architectures may perform differently, the architecture of LSTM network employed for the current work is discussed in the Section IV. Next, in step 2-3, the predicted indices are compared to the real ones through the observation of probability mass functions (PMFs) and histograms as illustrated in Fig. 3. In step 4, a penalty function is defined to account for the error probability of each mapping combination. Finally, in step 5, a mapping function is defined based on upper bounding the sum probability of exceeding a given target BLER.

Algorithm 2: Definition of CQI corrections Algorithm

1 Perform SINR prediction on a historical data set and convert the predicted and real SINR values to the corresponding CQI index as in Fig. 2;

2 Evaluate the empirical PMFs for each CQI index within the prediction $p_{\text{CQI}_p}(x) = \Pr(\text{CQI}_p = x)$, where $x = \{0, 1, \ldots, 15\}$;

3 Evaluate the empirical conditional PMFs of the real CQI indices y given the corresponding CQI indices x as $p_{\text{CQI}_r}(y|x) = \Pr(\text{CQI}_r = y|x)$;

4 Evaluate the penalty for each possible correction: Penalty= $\Pr(\text{CQI}_p = x_i) \times \sum_{i=1}^{y-1} \Pr(\text{CQI}_r = i|x)$;

5 Define a mapping function given that the sum penalty is upper bounded by the target BLER;
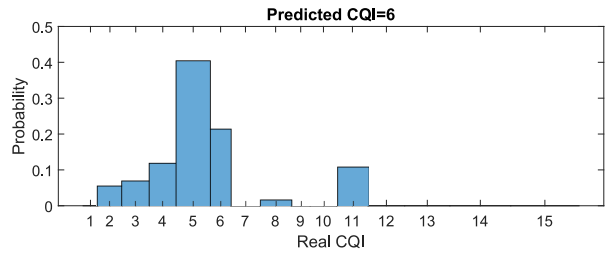

Fig. 3: Actual CQI when LSTM prediction corresponds to CQI= 6, i.e., $\Pr(\text{CQI}_r = y|x = 6)$ for $y = 0, \ldots, 15$.

B. Interference aware semi-coordinated scheduling

As discussed earlier, the baseline scheduling approach assumes uncoordinated gNBs. In contrast, perfect coordination is possible only when all available information is exchanged between gNBs or a centralised scheduler takes global decisions. To reduce the overhead of the optimal fully coordinated scheduling, a semi-coordinated scheduler is proposed in this section. It runs *independently* on each gNB, but still leverages interference awareness by scheduling UEs in groups of low cross-interference. In detail, the proposed scheduling approach creates groups of UEs attached to different gNBs based on the average SINR measured during concurrent transmissions, i.e., the learned cross-interference patterns. The semi-coordinated scheduler boils down to a simple rule: *gNBs will transmit to UEs from a single group at any given time slot.*

The group membership is defined such that the average SINR of all groups is maximized. Assuming K subgroups for the set of UEs $\mathcal{J}$, denoted by $\mathcal{J}_1, \ldots, \mathcal{J}_K$ with $\cup_{k=1}^{K} \mathcal{J}_k = \mathcal{J}$, memberships are defined as $j \in \mathcal{J}_k, k = 1 \ldots, K$ by solving the following optimization problem

$$\max_{k \in \{1, \ldots, K\}, j \in \mathcal{J}_k} \sum_{i \in \mathcal{I}} \sum_{k \in \{1, \ldots, K\}} \sum_{j \in \mathcal{J}_k} SINR_j^{(i)} \quad (5)$$

$$\text{s.t.} \quad (3), (4), \cup_{k=1}^{K} \mathcal{J}_k = \mathcal{J}, \lfloor \mathcal{J}_k \rfloor \leq J/K \leq \lceil \mathcal{J}_k \rceil,$$

where the last constraint ensures that the sizes of the subgroups are roughly equal to reduce queue lengths. For each possible grouping, there will be $M = K - J + K \lfloor J/K \rfloor$ subgroups of $\lfloor J/K \rfloor$ elements and $L = J - M$ subgroups of $\lceil J/K \rceil$
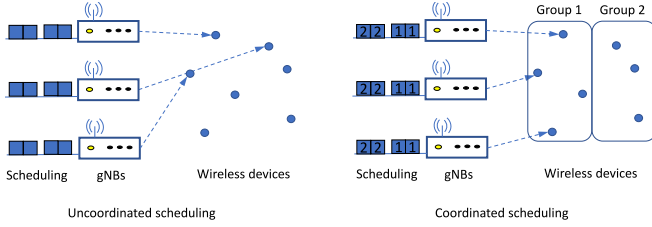
Fig. 4: Scheduling scenarios.

TABLE I: Architecture of the LSTM predictor.

Number of hidden layers	2
Neurons per layer	64 and 32
Optimizer	Adam
Regularizer	$L2$
Learning rate	0.0001

elements, with $\lfloor \cdot \rfloor$ and $\lceil \cdot \rceil$ denoting the floor and ceiling functions respectively. It can be deduced that the search space size for the grouping optimization problem is given by the multinomial coefficient $\frac{J!}{(\lfloor J/K \rfloor!)^M (\lceil J/K \rceil!)^L M! L!}$. With respect to determining K, it can be found by sequential search and set to the maximum value that generates non-empty subgroups. Once the group memberships have been found, the gNBs coordinate transmissions to a single group at a time. The proposed approach is evaluated in Section IV.

IV. NUMERICAL EVALUATION

To illustrate the performance gains of the proposed approach, the achievable SE of the semi-coordinated scheduling with smart LA is compared to a benchmark uncoordinated scheduler (with or without LA). Fig. 4 illustrates both uncoordinated and interference aware scheduling. In the former each gNB takes independent scheduling decisions as dictated by proportional fairness, discussed in Section II; in the latter scheduling is performed on a group membership basis as discussed in Section III-B.

In the simulated scenario, a network consisting of $I = 3$ gNBs and $J = 15$ UEs randomly located in a factory hall of size $50\text{m} \times 30\text{m}$ with gNBs attached to the walls is considered. To better evaluate the practicality of the proposed solution it is assumed that 2 of the UEs are moving on deterministic trajectories within the hall with speed of 5m/s causing additional variations to the experienced SINR. It is considered that the transmit power of the gNBs is fixed to 24dBm and each has a uniform linear array of $N = 8$ uniformly spaced identical antenna elements of equal magnitude and linearly progressive phase from element to element. Finally, the gNBs are assumed to be equipped with single antenna panels (this study does not consider multi-user MIMO transmissions).

The LSTM predictor was trained using a dataset of 8×10^4 SINR measurements at each UE. The architecture of the predictor is summarized in Table I. Due to low number of features in the dataset, the number of hidden layers and neurons per layer are equal to 2 and $(64, 32)$, respectively; it was observed that larger architectures did not improve the accuracy. Furthermore, an $L2$ regularizer is used to avoid overfitting. The LSTM output is subsequently converted to CQI indices using the CQI mapping described in the previous section; finally the MCSs are adjusted accordingly.

TABLE II: SINR level in dB measured at UEs attached to gNB2, while gNB1 (yellow) and gNB3 (blue) are active.

UEs attached to gNB2									
15	12.2	13.4	15.3	20.6	14.2	12.3	15.4	10.8	10.4
11	1.2	4.1	12.3	6.4	10.0	2.9	5.9	4.4	16.0
8	4.8	7.3	8.8	18.7	7.8	5.6	8.6	5.9	7.5
3	3.4	6.2	8.7	15.6	7.7	5.8	8.8	12.5	3.9
2	5.1	8.7	8.4	13.1	7.4	5.9	8.9	7.7	2.2
1	10.9	12.3	16.6	19.4	15.4	13.1	16.2	17.3	3.1
	4	5	6	7	9	10	12	13	14
UEs attached to gNB1 and gNB3									
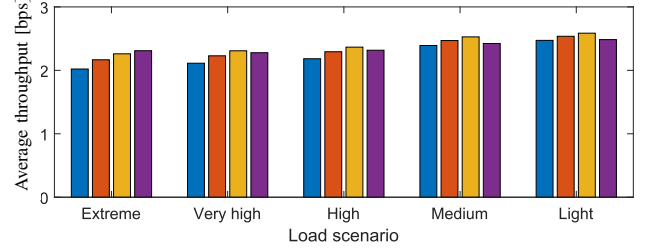
a) Average throughput vs different cases of buffer overflow.
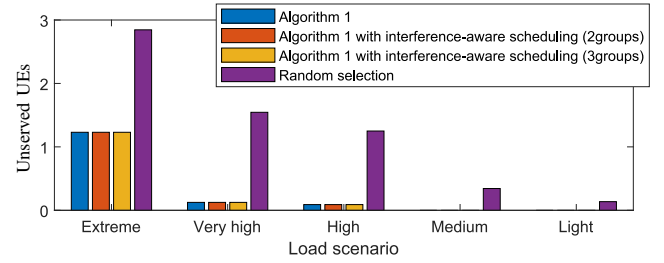
b) Average number of unserved UEs vs different cases of buffer overflow.

Fig. 5: Evaluation of the proposed smart LA.

To provide an example for the proposed interference aware semi-coordinated scheduling, average SINR values experienced at UEs attached to gNB 2 (shown on the vertical axis), is depicted in Table II. In each column the UEs attached to gNB 1 (shown in yellow) and gNB 3 (shown in blue) are depicted. It is observed that the link gNB 3 - UE 4 highly impacts the SINR at UE 11 with the average SINR level of the latter decreasing to approximately 1dB. Similar cross-interference tables can be generated for gNB 1 and gNB 3. Note that, due to the assumption that a particular gNB can serve only one UE at a time, there is no cross-interference between UEs attached to the same gNB. Finally, UEs are divided into groups by solving problem (5).

A. Evaluation of the proposed UE attachment algorithm

Using the system parameters described above, the advantage of using the proposed attachment heuristic, given in Algorithm 1, is shown. Figures 5(a) and (b) illustrate the average throughput and the number of unserved UEs due to buffer overflows, respectively. Four scenarios are depicted: 1) random selection, i.e., uncoordinated scheduling where the selection of unserved UEs is performed in a randomly; 2) Algorithm 1, i.e., uncoordinated scheduling, however selection of unserved UEs is performed based on the steps described in Algorithm 1; 3) and 4) Combination between Algorithm 1 and the proposed interference-aware scheduling with 2 and 3 groups of UEs, respectively. The figures show the average throughput assuming perfect knowledge of the SINR experienced at UEs, i.e., gNBs choose the optimal MCS in every time slot.

It is observed that by simply employing Algorithm 1 the number of unserved UEs drops considerably for a small cost in the throughput as compared to random selection. Examining the two figures jointly, it is clear that random selection is suboptimal as more UEs remain unserved (which might be beneficial when looking only at the throughput because of reduced cross-interference). This is most noticeable in the extreme case where random selection outperforms the proposed mechanisms in terms of average throughput, however, this is at the cost of substantial decrease in the served UEs. Next, it can be seen that in all other cases the combination of interference-aware scheduling and Algorithm 1 allows the system to avoid scheduling UEs with high cross-interference resulting in an improvement of the average throughput while keeping the number of unserved UEs small.

B. Evaluation of the proposed smart LA and scheduling

This section demonstrates the gains brought by each element of the proposed smart LA and scheduling. Fig. 6 shows the average SE for different levels of coordination and SINR knowledge at the gNBs. The system model consists of 15 UEs and SE is averaged over 10^5 time slots. First, in terms of coordination the following scenarios are differentiated: uncoordinated, i.e., decisions are entirely based on meeting proportional fairness; interference aware semi-coordinated with 2 or 3 groups, i.e., decisions are based on group membership as described in Section III-B. Next, in terms of SINR reporting three cases are distinguished: average SINR, where gNBs receive only periodic estimates of the SINR levels at UEs; SINR prediction, where gNBs rely on the proposed smart LA described in III-A; and perfect SINR, where gNBs have perfect SINR information.

It can be seen that any of the proposed techniques brings on its own an improvement to the SE. First, it is observed that the employment of the interference aware scheduling (3 groups) with average SINR, gives a 22% increase in the average SE, as compared to the baseline approach. Next, by including SINR prediction, a further improvement of 40% is observed, resulting in cumulative improvement of 62%. Based on the parameters given in [10], this increase shows that the average code rate increases from 308/1024 to 602/1024, i.e., it is roughly doubled. Finally, Fig. 6 shows that the proposed interference aware scheduling provides an improvement in the average SE also in the case of perfect SINR knowledge. While perfect knowledge of the SINR allows gNBs to optimally choose their MCS, interference aware scheduling eliminates high cross interference between UEs and this results in an additional 7% improvement in the average SE.

The numerical results show that indeed there is room for improvement in the currently employed baseline LA and scheduling approaches. The proposed approach provides an efficient trade-off between increasing the SE while keeping the overhead low; furthermore it reduces the cross-interference while increasing the number of served UEs, both of which play a role in efficient IIoT deployment. As a future work, we intend to improve the system model by including: UEs with different delay requirements, gNBs with multiple antenna panels and allow for frequency multiplexing between UEs.
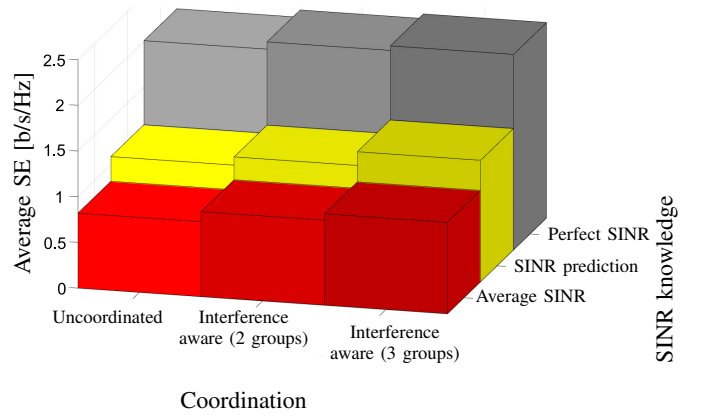

Fig. 6: Improvement in average SE by incorporating smart LA and interference aware scheduling.

V. CONCLUSIONS

In this work, a smart LA and scheduling framework for IIoT is proposed, including low complexity UE attachment, SINR prediction, CQI mapping, and UE grouping for interference avoidance in semi-coordinated scheduling. The gain of each of these mechanisms were demonstrated though numerical evaluations in a realistic scenario according to the 3GPP specs for IIoT networks. It was shown that the proposed solutions provide a 62% increase in average SE, compared to the currently used standard approach. Furthermore, employing the proposed scheme allows deployment of more UEs without increasing cross-interference levels. In future work, heterogeneous traffic and alternative ML tools such as 1D convolutional neural networks will be explored.

REFERENCES

[1] L. Wang, V. Wong, R. Schober, and D. Ng, *Key Technologies for 5G Wireless Systems*. UK: Cambridge University Press, Mar. 2017.

[2] S. Grimaldi, A. Mahmood, S. Hassan, M. Gidlund, and G. Hancke, "Autonomous interference mapping for industrial IoT networks over unlicensed bands," *IEEE Ind. Electron. Magazine*, 2020.

[3] F. Calabrese, C. Rosa, K. Pedersen, and P. Mogensen, "Performance of proportional fair frequency and time domain scheduling in LTE uplink," in *Eur. Wirel. Conf.*, 2009, pp. 271–275.

[4] 3GPP TS 22.104 V17.4.0, "Service requirements for cyber-physical control applications in vertical domains; Stage 1," 2020.

[5] A. Brighente, J. Mohammadi, and P. Baracca, "Interference distribution prediction for link adaptation in ultra-reliable low-latency communications," in *IEEE VTC2020-Spring*, 2020, pp. 1–7.

[6] S. Yin, D. Chen, Q. Zhang, M. Liu, and S. Li, "Mining spectrum usage data: A large-scale spectrum measurement study," *IEEE Trans. Mobile Comput.*, vol. 11, no. 6, pp. 1033–1046, 2012.

[7] T. Le and S. Moh, "Link scheduling algorithm with interference prediction for multiple mobile WBANs," *Sensors*, vol. 17, no. 10, 2017.

[8] 3GPP TS 38.901 V16.1.0, "Study on channel model for frequencies from 0.5 to 100 GHz," 2019.

[9] S. Mollahasani and E. Onur, "Density-aware, energy- and spectrum-efficient small cell scheduling," *IEEE Access*, vol. 7, pp. 65 852–65 869, 2019.

[10] 3GPP TS 38.214, "NR; Physical layer procedures for data," 2020.

[11] G. Pocovi, A. Esswie, and K. Pedersen, "Channel quality feedback enhancements for accurate URLLC link adaptation in 5G systems," in *IEEE VTC2020-Spring*, 2020, pp. 1–6.

[12] M. Hirzallah, M. Krunz, B. Kecicioglu, and B. Hamzeh, "5G new radio unlicensed: Challenges and evaluation," *IEEE Trans. on Cogni. Commun. and Networking*, vol. 7, no. 3, pp. 689–701, 2021.

[13] U. Challita, L. Dong, and W. Saad, "Proactive resource management for LTE in unlicensed spectrum: A deep learning perspective," *IEEE Trans. Wireless Commun.*, vol. 17, no. 7, pp. 4674–4689, 2018.